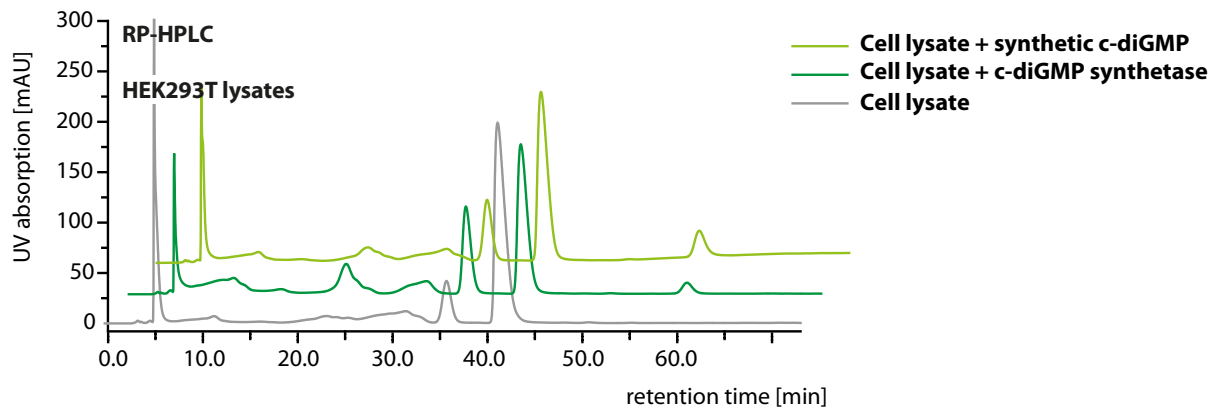
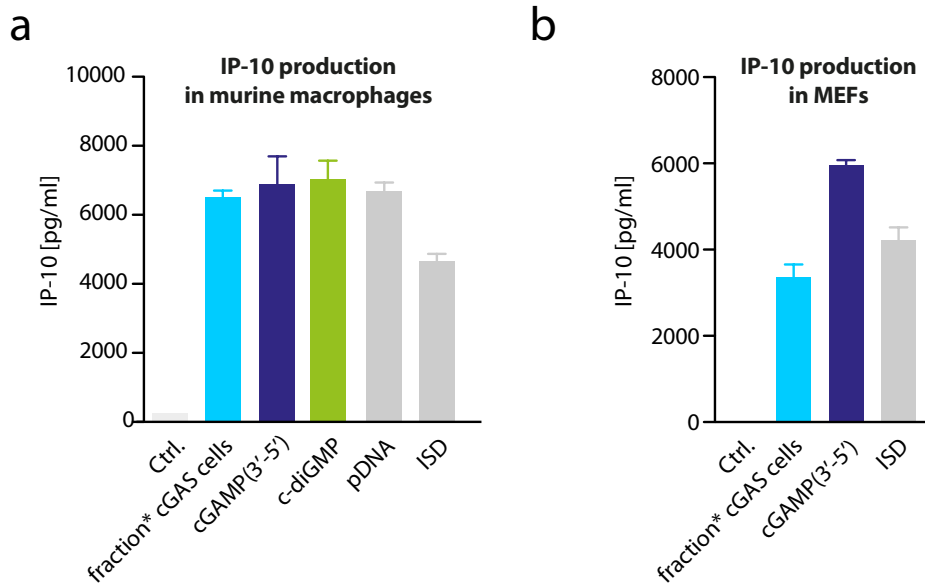


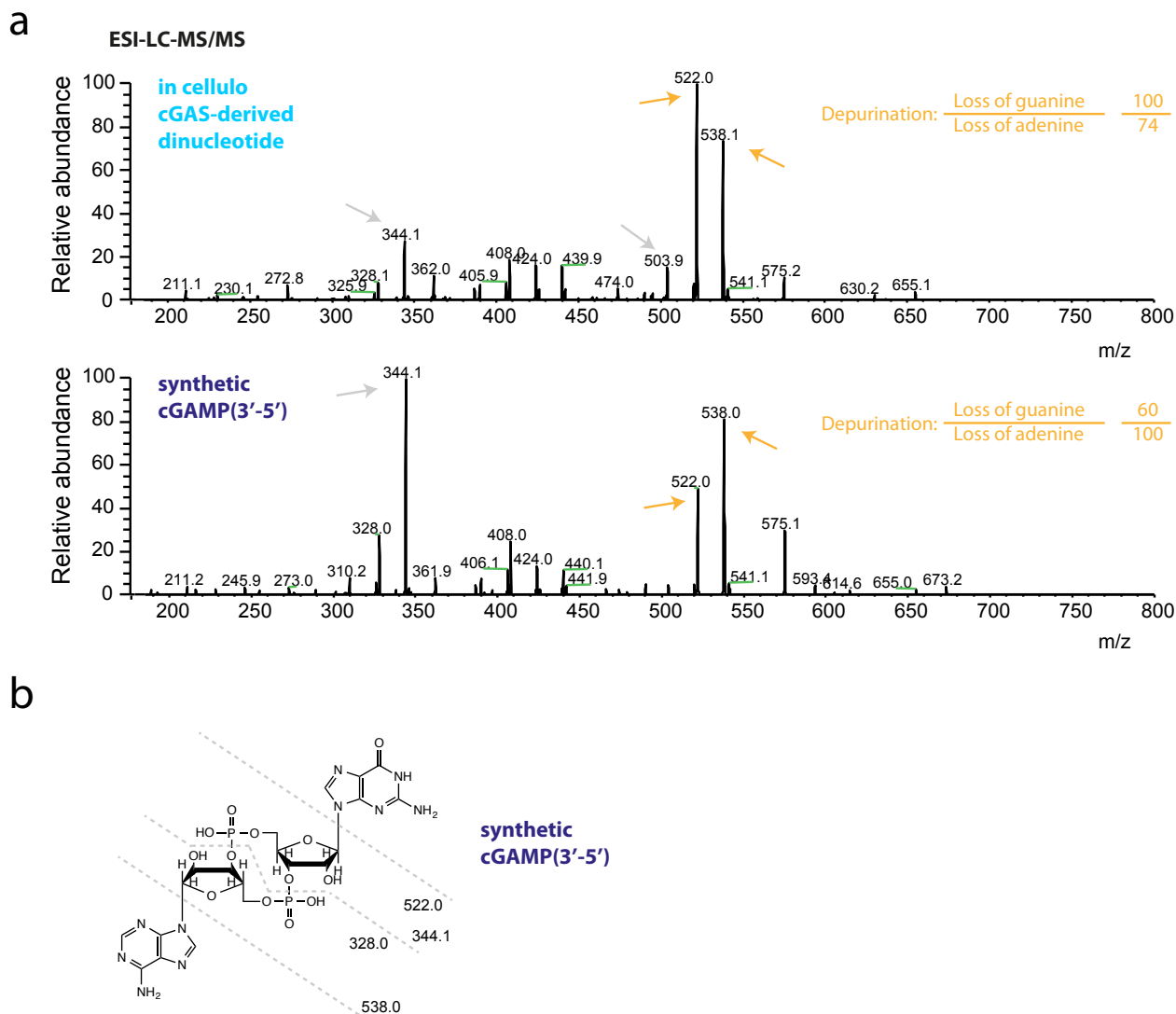
Supplementary Figure 1 | Expression analysis of wild type murine STING and the R231A mutant. Expression analysis of wild type murine STING and its mutant R231A (both harboring a GFP-Tag) by immunoblotting in HEK293T cells 16h after transfection. Immunoblot for β-Actin served as a control. Representative data out of two independent experiments are shown.



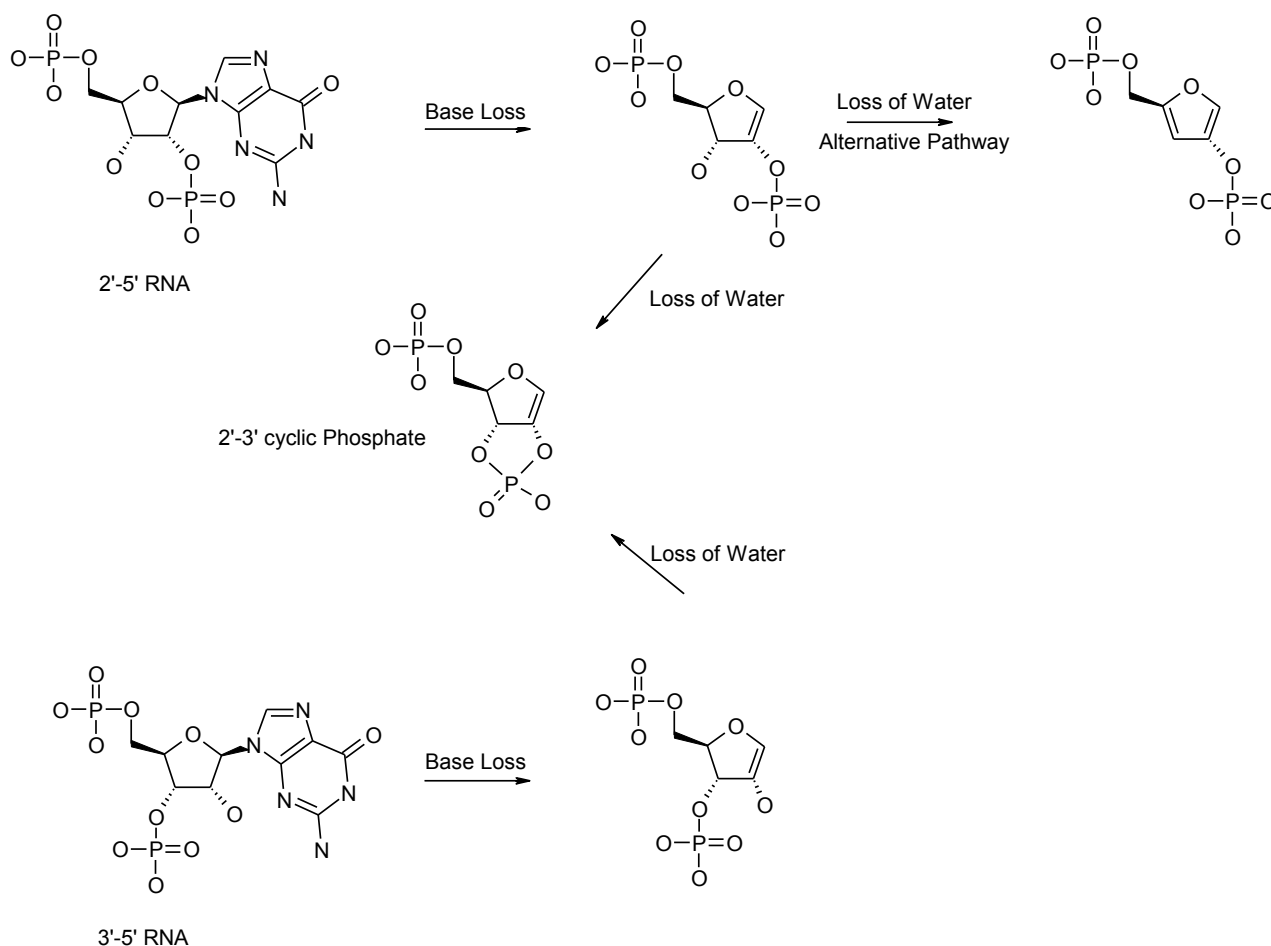
Supplementary Figure 2 | Overexpression of cyclic di-GMP synthetase induces endogenous expression of cyclic di-GMP in HEK293T cells. Chromatograms from purified lysates of untreated HEK293T cells (grey) and cyclic di-GMP synthetase overexpressing HEK293T cells (dark green) are shown together with synthetic cyclic di-GMP spiked into untreated HEK293T lysate (light green). Representative data out of two independent experiments are shown.



Supplementary Figure 3 | The endogenous cGAS product is a potent trigger of type I IFN response in BMDMs and MEFs. (a-b) BMDMs (a) and primary MEFs (b) were transfected with purified cGAS product extracted from HEK293T cells overexpressing cGAS, synthetic cGAMP(3'-5'), cyclic di-GMP, plasmid DNA and ISD. After 14h supernatants were collected and the production of IP-10 was assessed by ELISA. Representative data out of three independent experiments are shown as mean values + SEM.



Supplementary Figure 4 | Tandem mass spectrometry of the cGAS-derived product suggests the presence of a 2'-5' phosphodiester linkage. (a) Tandem MS spectra from in cellulo synthesized cGAS product (light blue) and synthetic cGAMP (3'-5') (dark blue) is shown. Grey arrows highlight an ion product with m/z 344.1, indicative of a nucleotide with 2'-3'-cyclic phosphates. Orange arrows highlight signals consistent with depurination of the dinucleotides (m/z 522.0 and m/z 538.1). Representative data out of three independent experiments are shown. (b) Expected fragmentation pathway of synthetic cGAMP(3'-5') is shown.



Supplementary Figure 5 | Tandem mass spectrometry fragmentation of 2'-5' vs. 3'-5' linked RNA.

Supplementary Note 1 | Analysis of tandem MS spectra suggests the presence of a 2'-5' phosphodiester bond within the cGAS-derived dinucleotide product.

The tandem MS² spectra of synthetic cGAMP(3'-5') and the cGAS-derived product isolated from cell culture lysates showed significant differences, when analyzed by tandem MS in negative ion mode. Among other differences, the cGAS-derived dinucleotide showed a higher propensity for depurination of the guanosine, indicative of a lower stability of the N-glycosidic bond at the ribose ring in comparison to the synthetic cGAMP(3'-5') molecule (Supplementary Figure 4). A likely scenario for this change in stability could be ascribed to a 2'-instead of 3'-phosphodiester bond at the ribose ring of the guanosine.

The fragmentation of 3'-5'-RNA mainly leads to the y- and c-fragments induced by a cleavage of a 5'-P-O bond^{1,2}. For a cyclic dinucleotide this fragmentation pathway will open the cyclic dinucleotide structure by forming a 2'-3'-cyclic phosphate, but it is mass neutral in the first step (Supplementary Figure 5). In a second fragmentation step the same fragmentation pathway will dissociate the dinucleotide in two nucleotides with 2'-3'-cyclic phosphates, with $m/z = 344$ (G) and $m/z = 328$ (A). The product ion with $m/z = 344$ was detected with highest abundance as the main fragmentation product of synthetic cGAMP with two 3'-5'-phosphodiester groups. This result is in sharp contrast to the spectrum obtained for the cGAS product isolated from cell lysate, with just 30% relative abundance for this product ion. These findings suggested a different configuration at the G-nucleotide in the synthetic cGAMP(3'-5') versus the *in cellulo* produced cGAS product.

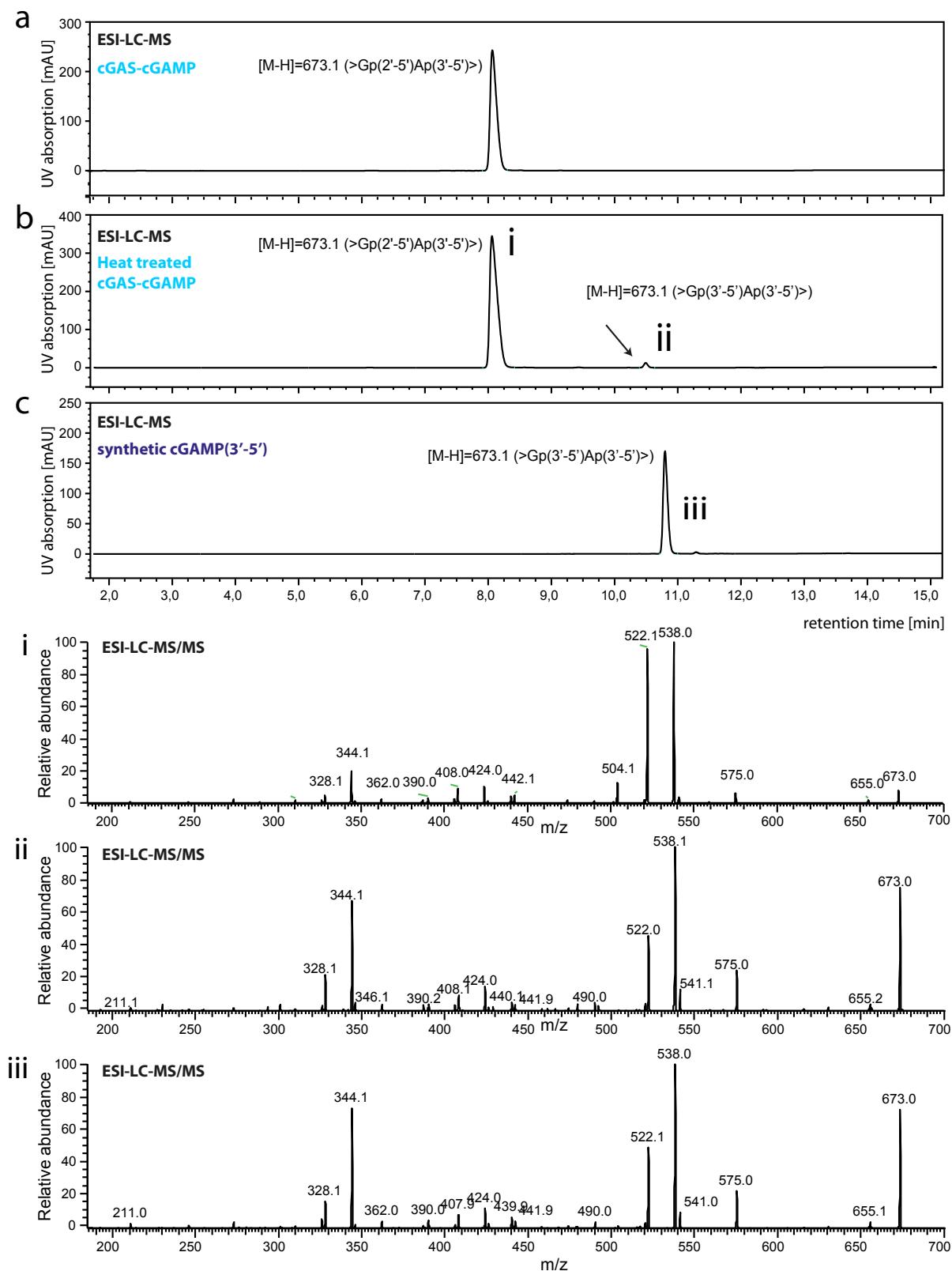
Another well-described fragmentation pathway of RNA is the neutral loss of a base that leads to the signals at $m/z = 538$ and $m/z = 522$, by forming a C1 to C2 double bond. Remarkably, for the synthetic cGAMP(3'-5') adenine is eliminated with a higher relative abundance compared to guanine, whereas the ratio is reversed in the dinucleotide isolated from cGAS overexpressing cells. It is known, that the 2'-hydroxy group has a stabilizing effect on the N-glycosidic bond in RNA^{3,4}. But in the case the 2'-hydroxy group is changed to 2'-phosphoester bond the stabilizing effect becomes lost and the neutral base loss of guanine should significantly increase.

Additional evidence for a guanosine 2'-phosphodiester is the strongly increased neutral loss of water in the cGAS-derived substance after elimination of the guanine base ($m/z = 522$ to $m/z = 504$ in the tandem MS³ spectrum of $m/z = 522$; data not shown). The significantly higher loss of water in the natural compound over the synthetic reference was also observed by Wu et al.⁵, but not attributed to different structures. For a 2'-5'-phosphodiester nucleotide bond two different pathways are possible for the loss of a water molecule after base elimination. The first pathway is similar between 2'-5' and 3'-5' RNA, where water is eliminated by forming a cyclic phosphate between the free 2'- or 3'-hydroxy and the adjacent phosphodiester. The alternative pathway is unique to the 2'-5' RNA, where water can be eliminated from C3/C4 by forming another double bond and generating a thermodynamically stable aromatic furan ring (Supplementary Figure 4). No differences were found for the elimination of water after neutral loss of adenine, which supports a similar configuration in both compounds at the adenosine nucleotide.

All in all, these mass spectrometry findings strongly support the concept of a cyclic dinucleotide structure with guanosine connected 2' via a phosphodiester to 5'-adenosine and adenosine connected 3' via a phosphodiester to 5'-guanosine.

References

- 1 Andersen, T. E., Kirpekar, F. & Haselmann, K. F. RNA fragmentation in MALDI mass spectrometry studied by H/D-exchange: mechanisms of general applicability to nucleic acids. *J Am Soc Mass Spectrom* **17**, 1353-1368, doi:10.1016/j.jasms.2006.05.018 (2006).
- 2 Schurch, S., Bernal-Mendez, E. & Leumann, C. J. Electrospray tandem mass spectrometry of mixed-sequence RNA/DNA oligonucleotides. *J Am Soc Mass Spectrom* **13**, 936-945, doi:10.1016/S1044-0305(02)00413-0 (2002).
- 3 Tang, W., Zhu, L. & Smith, L. M. Controlling DNA Fragmentation in MALDI-MS by Chemical Modification. *Anal Chem* **69**, 302-312, doi:10.1021/ac960865o (1997).
- 4 Griffey, R. H., Greig, M. J., An, H., Sasmor, H. & Manalili, S. Targeted Site-Specific Gas-Phase Cleavage of Oligoribonucleotides. Application in Mass Spectrometry-Based Identification of Ligand Binding Sites. *Journal of the American Chemical Society* **121**, 474-475, doi:10.1021/ja983131x (1998).
- 5 Sun, L., Wu, J., Du, F., Chen, X. & Chen, Z. J. Cyclic GMP-AMP synthase is a cytosolic DNA sensor that activates the type I interferon pathway. *Science* **339**, 786-791, doi:10.1126/science.1232458 (2013).



Supplementary Figure 6 | The endogenous cGAS product isomerizes at high temperature to cGAMP(3'-5'). (a-c) Chromatograms from in cellulo synthesized cGAS product (a), heat-treated in cellulo synthesized cGAS product (b) and synthetic cGAMP(3'-5') (c) are shown. Tandem MS spectra of elution peaks from (b) (i and ii) and (c) (iii) are depicted. Representative data out of two independent experiments are shown.

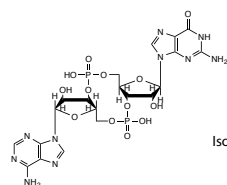
Supplementary Note 2 | The cGAS-derived dinucleotide product can isomerize into cGAMP(3'-5') at high temperature

Interestingly, upon prolonged incubation at high temperature (90°), a small, but consistent fraction of the cGAS-derived dinucleotide product converted into a molecule with identical retention time in RP-HPLC as well as an identical MS/MS fragmentation pattern as the synthetic cGAMP(3'-5') (Supplementary Figure 6). These data strongly suggested that the cGAS derived molecule and synthetic cGAMP(3'-5') were structural isomers with different phosphodiester linkages, being consistent with the idea of the cGAS-derived product harboring a 2'-5' phosphodiester linkage that could isomerize into a 3'-5' phosphodiester bond¹.

References

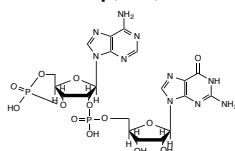
- 1 Seiffert, S. *et al.* Characterization of side reactions during the annealing of small interfering RNAs. *Anal Biochem* **414**, 47-57, doi:10.1016/j.ab.2011.02.040 (2011).

1 >Gp(3'-5')Ap(3'-5')>



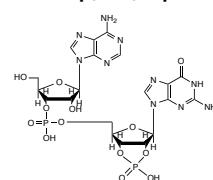
RNase T1 **ApGp**
 RNase T2 **Ap, Gp**
 S1 Nuclease **pA, pG**
 SVPDE **None**
 Isomerization to cGAMP **N/A**
 Periodate reaction **negative**

5 cAMPp(2'-5')G



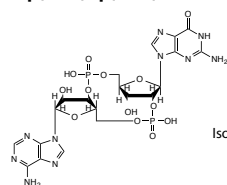
RNase T1 **None**
 RNase T2 **None**
 S1 Nuclease **None**
 SVPDE **cAMP, pG**
 Isomerization to cGAMP **no**
 Periodate reaction **positive**

9 Ap(3'-5')G>p



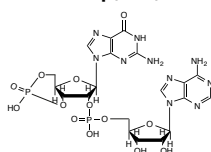
RNase T1 **None**
 RNase T2 **Ap, G>p**
 S1 Nuclease **A, pG>p**
 SVPDE **None**
 Isomerization to cGAMP **no**
 Periodate reaction **negative**

2 >Gp(2'-5')Ap(3'-5')>



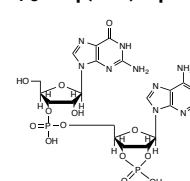
RNase T1 **None**
 RNase T2 **GpAp**
 S1 Nuclease **pGpA**
 SVPDE **pG, pA**
 Isomerization to cGAMP **yes**
 Periodate reaction **negative**

6 cGMPp(2'-5')A



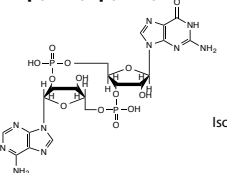
RNase T1 **None**
 RNase T2 **None**
 S1 Nuclease **None**
 SVPDE **cGMP, pA**
 Isomerization to cGAMP **no**
 Periodate reaction **positive**

10 Gp(3'-5')A>p



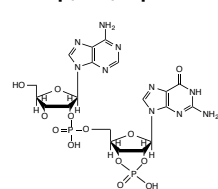
RNase T1 **Gp, A>p**
 RNase T2 **Gp, A>p**
 S1 Nuclease **G, pA>a**
 SVPDE **None**
 Isomerization to cGAMP **no**
 Periodate reaction **negative**

3 >Gp(3'-5')Ap(2'-5')>



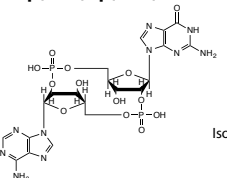
RNase T1 **ApGp**
 RNase T2 **ApGp**
 S1 Nuclease **pApG**
 SVPDE **pG, pA**
 Isomerization to cGAMP **yes**
 Periodate reaction **negative**

7 Ap(2'-5')G>p



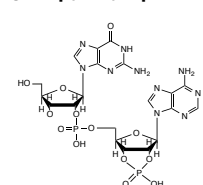
RNase T1 **None**
 RNase T2 **None**
 S1 Nuclease **None**
 SVPDE **None**
 Isomerization to cGAMP **no**
 Periodate reaction **negative**

4 >Gp(2'-5')Ap(2'-5')>



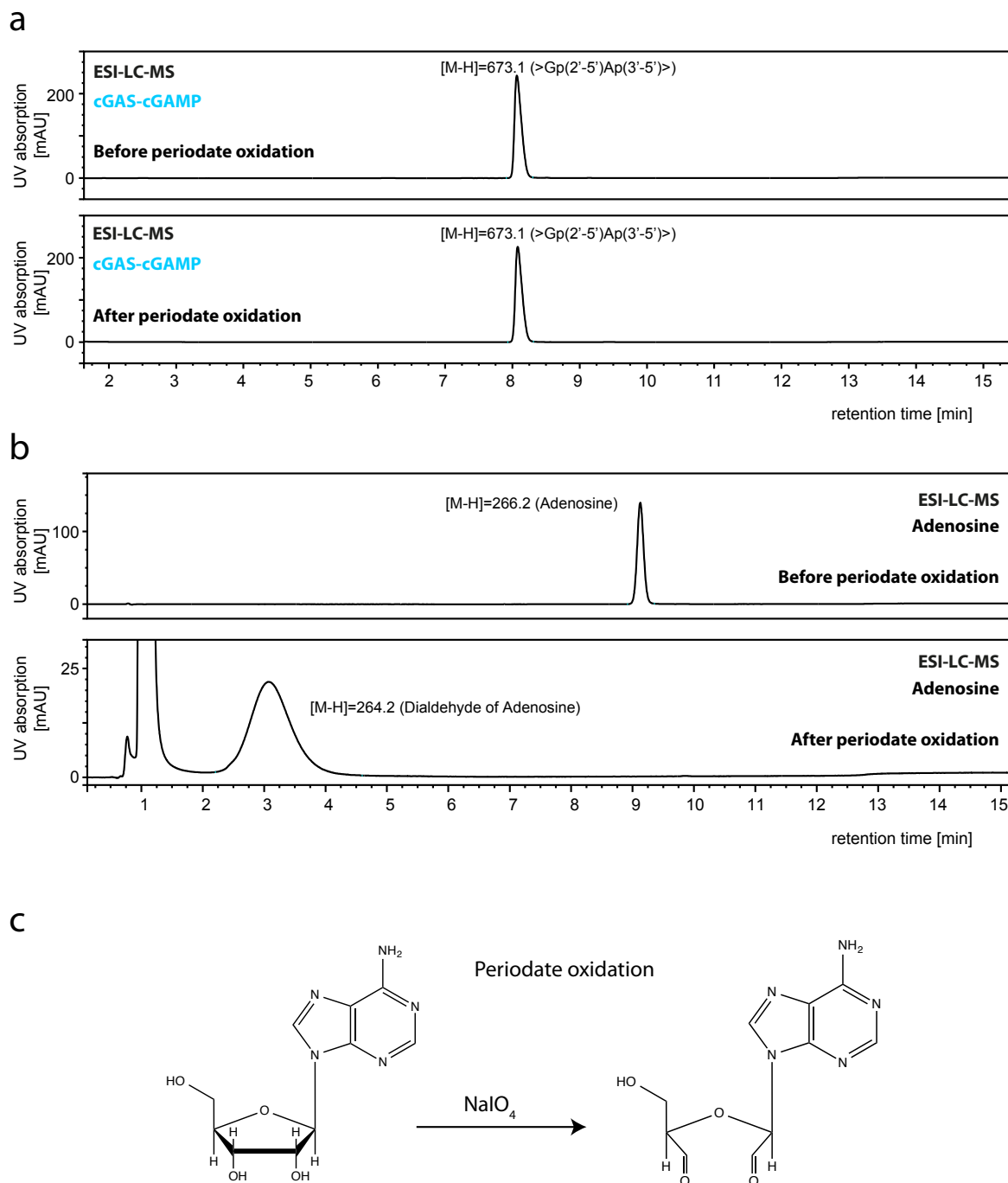
RNase T1 **None**
 RNase T2 **None**
 S1 Nuclease **None**
 SVPDE **pG, pA**
 Isomerization to cGAMP **yes**
 Periodate reaction **negative**

8 Gp(2'-5')A>p

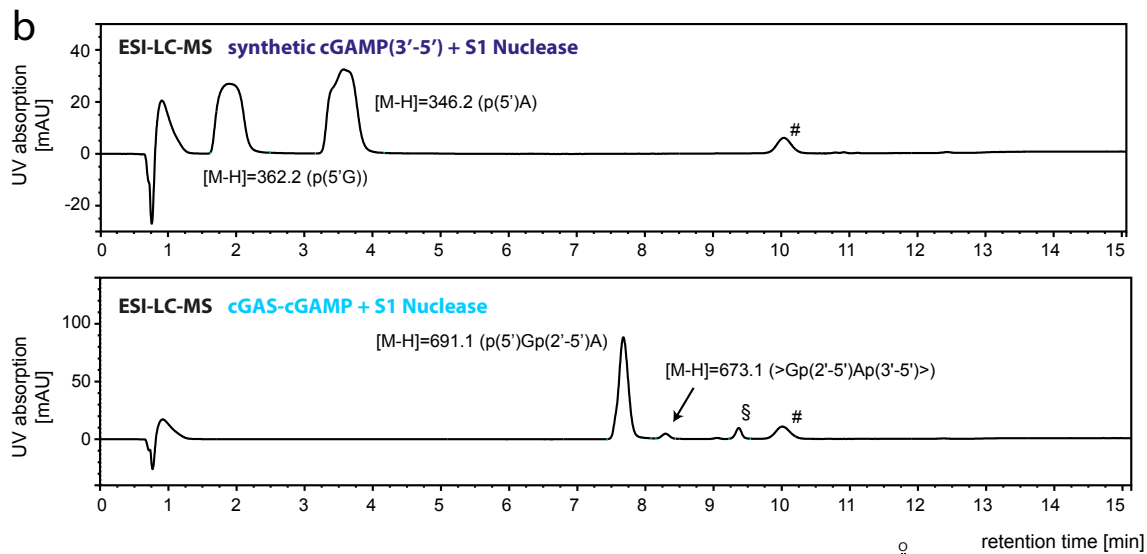
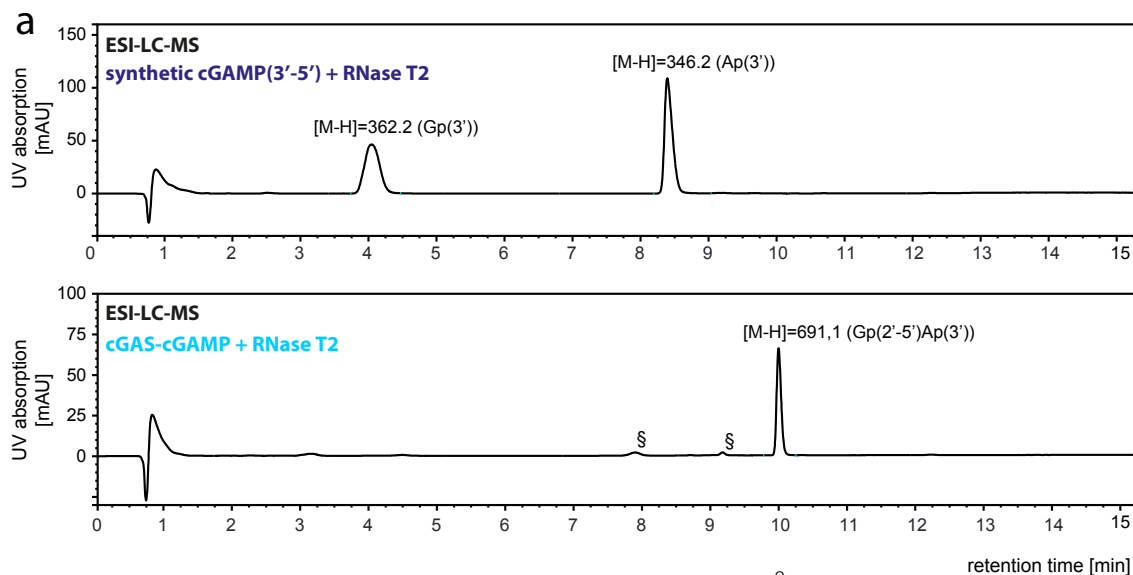


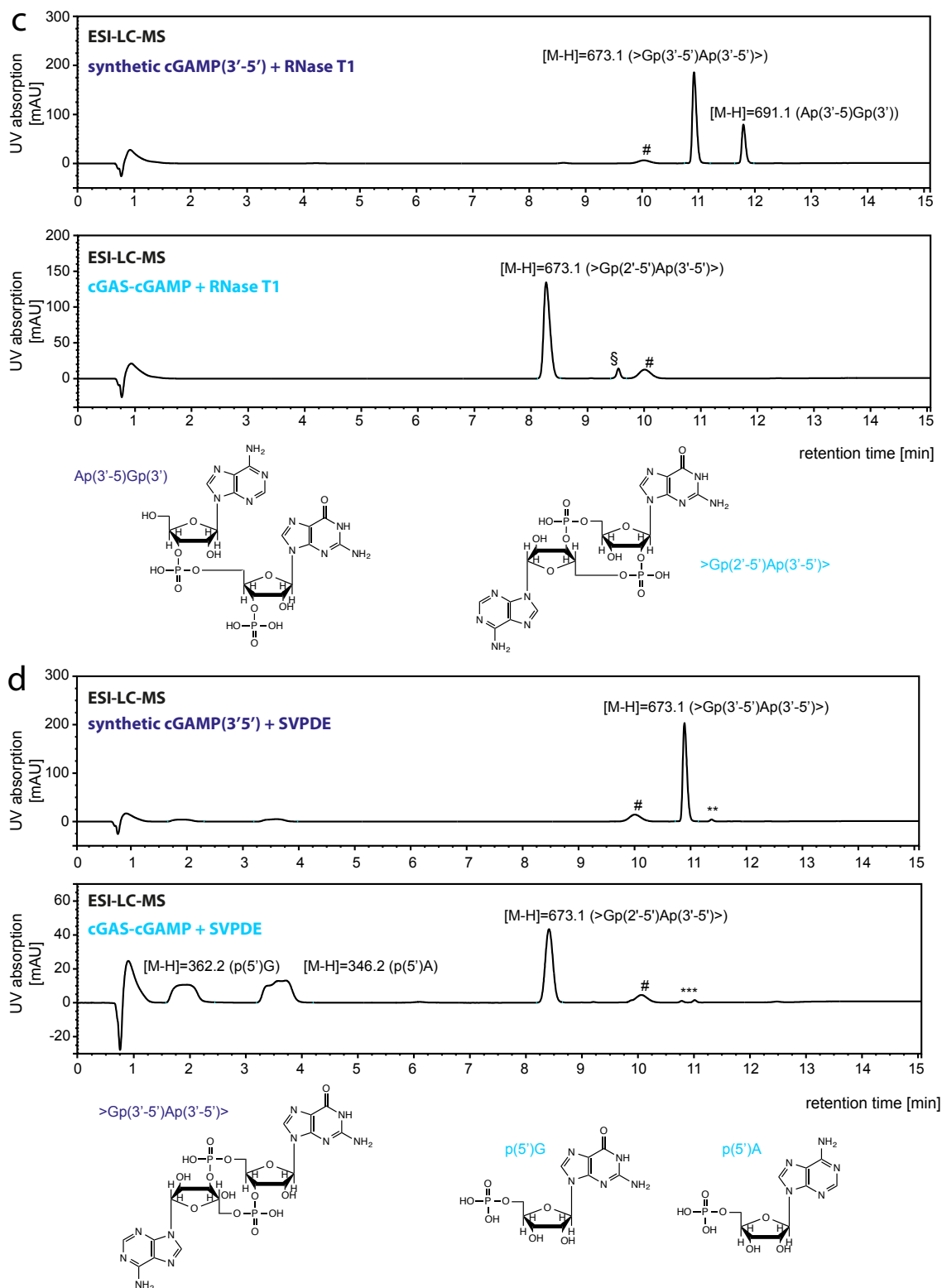
RNase T1 **None**
 RNase T2 **None**
 S1 Nuclease **None**
 SVPDE **None**
 Isomerization to cGAMP **no**
 Periodate reaction **negative**

Supplementary Figure 7 | Candidate products of cGAS. A schematic overview of candidate molecules consistent with the LC-MS-determined molecular mass of the endogenous cGAS product is depicted. Expected products upon incubation with the indicated enzymes are listed. cGAMP(2'-5') is highlighted in yellow.

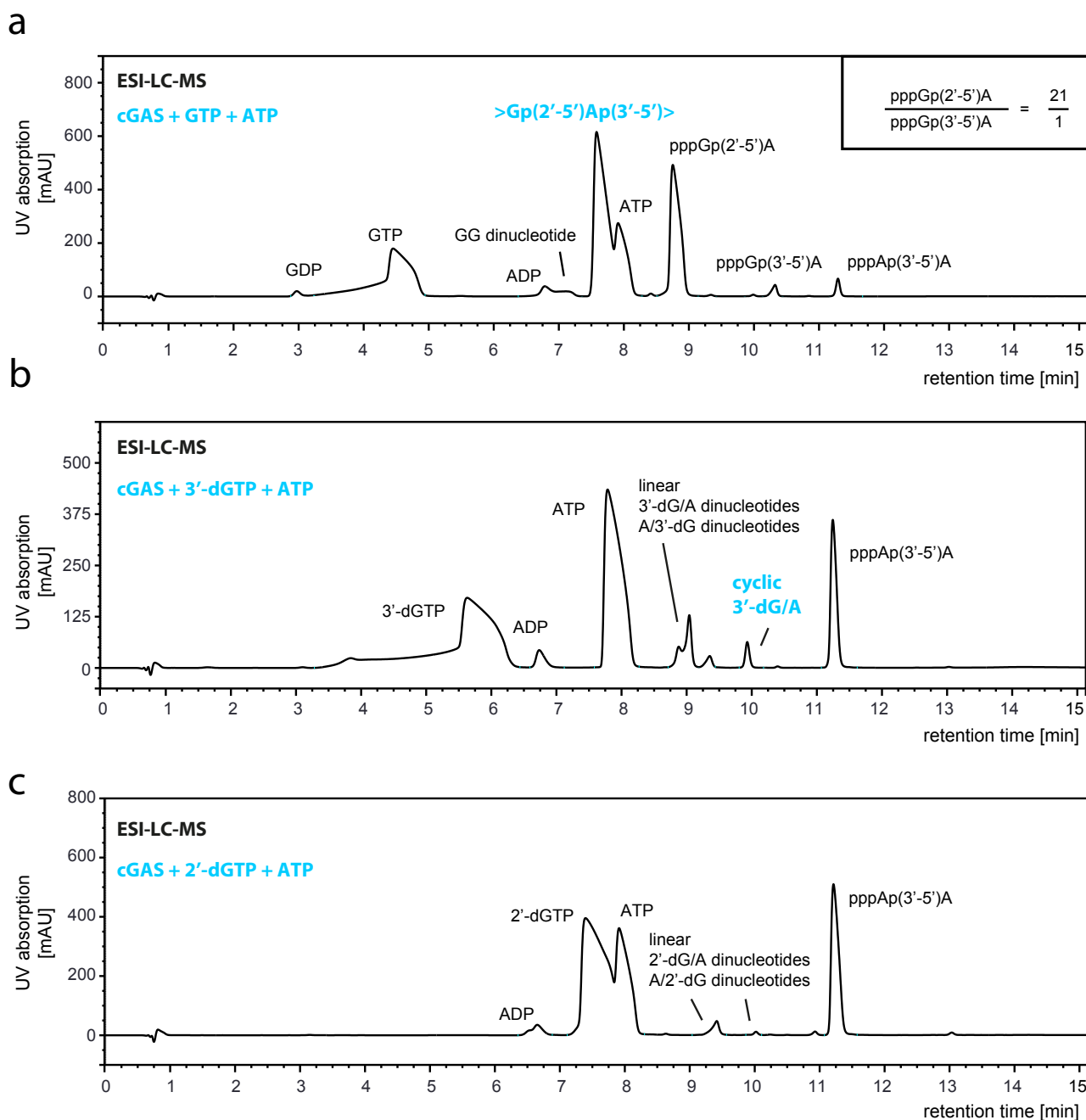


Supplementary Figure 8 | Negative periodate oxidation rules out the presence of free OH-groups at the 2' and 3' terminal positions. (a) Chromatograms from in cellulo synthesized cGAS product before and after periodate oxidation are shown. (b) Chromatograms from adenosine before and after periodate oxidation are shown. (c) Schematic view of the reaction pathway of periodate oxidation is depicted. Representative data out of two independent experiments are shown.





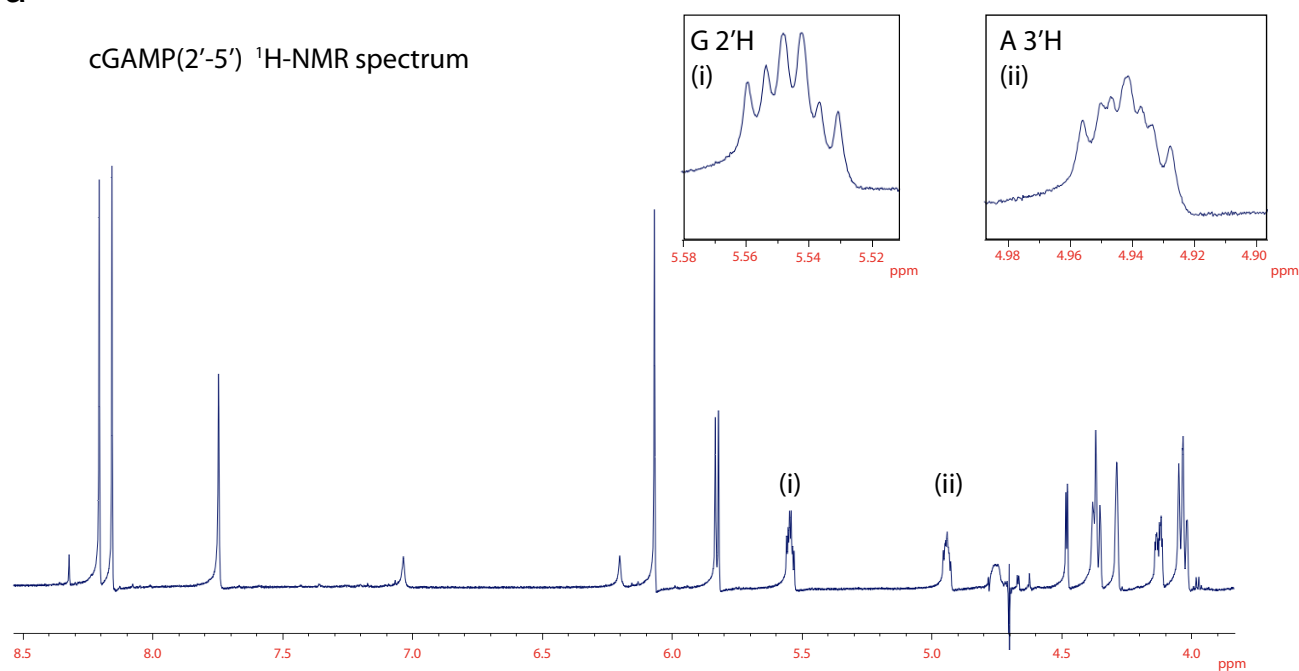
Supplementary Figure 9 | Enzymatic assays reveal the endogenous cGAS product to be (>Gp(2'-5')Ap(3'-5')>). (a) Chromatograms and schematic view of the reaction products from (a) RNase T2, (b) S1 Nuclease, (c) RNase T1 and (d) SVPDE digestion of synthetic cGAMP(3'-5') (dark blue) and in cellulo synthesized cGAS product (light blue). Representative data out of two independent experiments are shown. Peaks marked with #, §, ** and *** represent phenol contamination, not assignable peaks (no ESI-MS signal), chemical synthesis by-products and isomerization products, respectively.



Supplementary Figure 10 | GTP, 3'-dGTP and 2'-dGTP lead to distinct cGAS reaction product profiles.

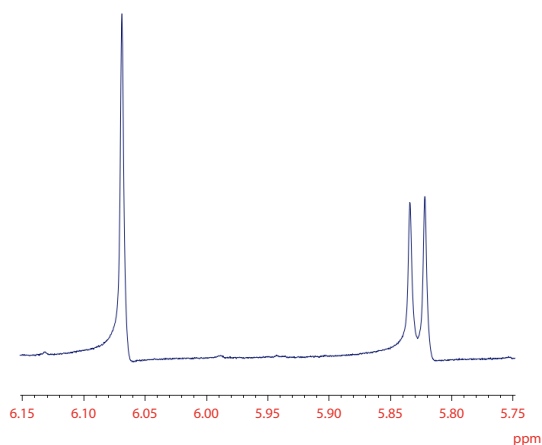
(a-c) Chromatograms of in vitro cGAS enzymatic reaction products with ATP and GTP (a), 3'-dGTP (b) or 2'-dGTP (c) are shown. The assignment of peaks to mono- and dinucleotide species was assessed by LC-MS. In case of arguable isomers, characterization of peaks was complemented with enzymatic digestion analysis for the crucial components. The panel in the upper right of the cGAS/ATP/GTP reaction (a) illustrates the relative ratio of the abundance of pppGp(2'-5')A vs. pppGp(3'-5')A. Data are representative of n=2 experiments.

a

cGAMP(2'-5') ^1H -NMR spectrum

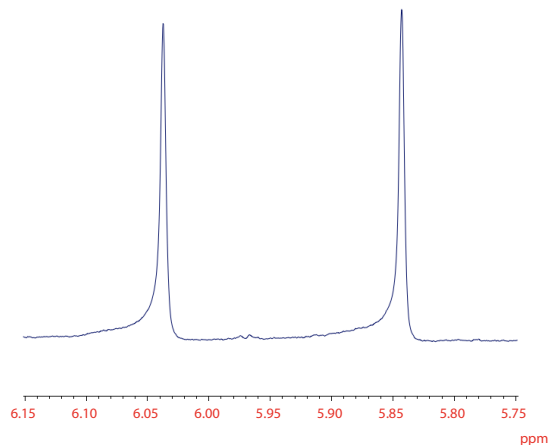
b

cGAMP(2'-5')



c

cGAMP(3'-5')



Supplementary Figure 11 | Characterization of cGAMP(2'-5') and cGAMP(3'-5') by ^1H -NMR spectroscopy. (a) The complete ^1H -NMR spectrum of the in vitro reaction product of cGAS (cGAMP(2'-5')) is shown. The inserts in the top indicate the expanded G 2'H (i) and A 3'H (ii) regions. (b and c) Close-up view of the ^1H regions of the ^1H -NMR spectrum of cGAMP(2'-5') (b) and cGAMP(3'-5') (c).

Supplementary Note 3 | Characterization of cGAMP(2'-5') and cGAMP(3'-5') by ¹H-NMR spectroscopy

¹H-NMR spectrum of the cGAS synthase reaction product (Supplementary Figure 11a) was measured from a 0.1 mM solution in D₂O at 700 MHz. Singlets of the base protons indicated that no multimerization occurs under such conditions¹. The spectral parameters were determined as follows (700 MHz; D₂O): 8.2 (1H, s, A-H8); 8.16 (1H, s, A-H2); 7.75 (1H, s, G-H8); 6.07 (1H, s, A-H1', $J_{1'2'} = 0$ Hz); 5.83 (1H, s, G-H1', $J_{1'2'} = 8.49$ Hz); 5.55 (1H, m, G-H2', $J_{1'2'} = 8.49$ Hz, $J_{2'P} = 9.0$ Hz, $J_{2'3'} = 4.06$ Hz); 4.94 (1H, m, A-H3', $J_{2'3'} = 4.06$ Hz, $J_{3'P} = 6.7$ Hz, $J_{3'4'} = 10$ Hz); 4.75* (s); 4.48 (1H, d, A-H2', $J_{1'2'} = 0$ Hz, $J_{2'3'} = 4.06$ Hz); 4.37-4.07* (unresolved m, A and G 4' H and 5', 5'' H).

Comparison of the H-1' regions of the ¹H-NMR spectra of >Gp(2'-5')Ap(3'-5')> and >Gp(3'-5')Ap(3'-5')> revealed that the ribose of the 2'-5' linked guanosine preferentially occupies a 2'-endo conformation ($J_{(1'H-2'H)} = 8.49$ Hz)^{2,3} (Supplementary Figure 11b and c), whereas the singlet of the other ribose 1'H indicates the presence of an 3'-endo sugar for adenosine, similarly to the sugar pucker observed in the 3'-5',3'-5' cGAMP isomer⁴. The distinction between adenosine and guanosine 1'H signals is based on the fact that 1'H signals of adenosine 5', 3' and 2' monophosphates appear always downfield from the corresponding 1'H positions of the corresponding guanosine monophosphates, with no overlap observed between A and G series^{5,6}. Of note, this trend is also valid for the recently characterized cyclic 3'-5' GA diphosphates⁴.

The significantly different $J_{1'2'}$ coupling constants for G and A allows further distinctions between some neighboring atoms the following way: Two signals in the spectrum at 5.55 ppm and at 4.94 ppm show significant downfield shift compared to the standard positions of A and G 2' or 3' protons. These values indicate the presence of O-phosphoryl groups at the corresponding positions. Based on literature data for G and A 2' and 3' monophosphates⁵ the most downfield 5.55 ppm peak may result from H2' signals of 2'-GMP or 2'-AMP type environments. 2'-AMP can be eliminated based on analysis of the fine structure of the 5.55 ppm peak. This spin system could be modeled with good precision using $J_{1'2'} = 8.49$ Hz, $J_{2'P} = 9.0$ Hz, $J_{2'3'} = 4.06$ Hz parameters i.e. the 5.55 peak could be assigned to the guanosine having a 1'H proton with $J_{1'2'} = 8.49$ Hz. In this calculation literature $J_{2'P}$ values for nucleoside 2' phosphate esters were employed⁷.

The 4.94 ppm multiplet could be modeled with the following parameters: $J_{2'3'} = 4.06$ Hz, $J_{3'P} = 6.7$ Hz, $J_{3'4'} = 10$ Hz thus excluding 2'-H of adenosine, which shows no $J_{1'2'}$ coupling thus suggesting that this proton is attached to adenosine 3'C. $J_{(3,4)}$ was derived using the ($J_{3'4'} + J_{1'2'} = 10$ Hz relationship³.

For the residual 4 - 4.8 ppm region containing signals for 4'H, 5'CH₂ and the remaining ribose protons, partial overlap with the HDO background signal and the complex unresolved multiplets for the 5' and 5'' CH₂ protons allowed only a tentative assignments (These peaks are marked with *).

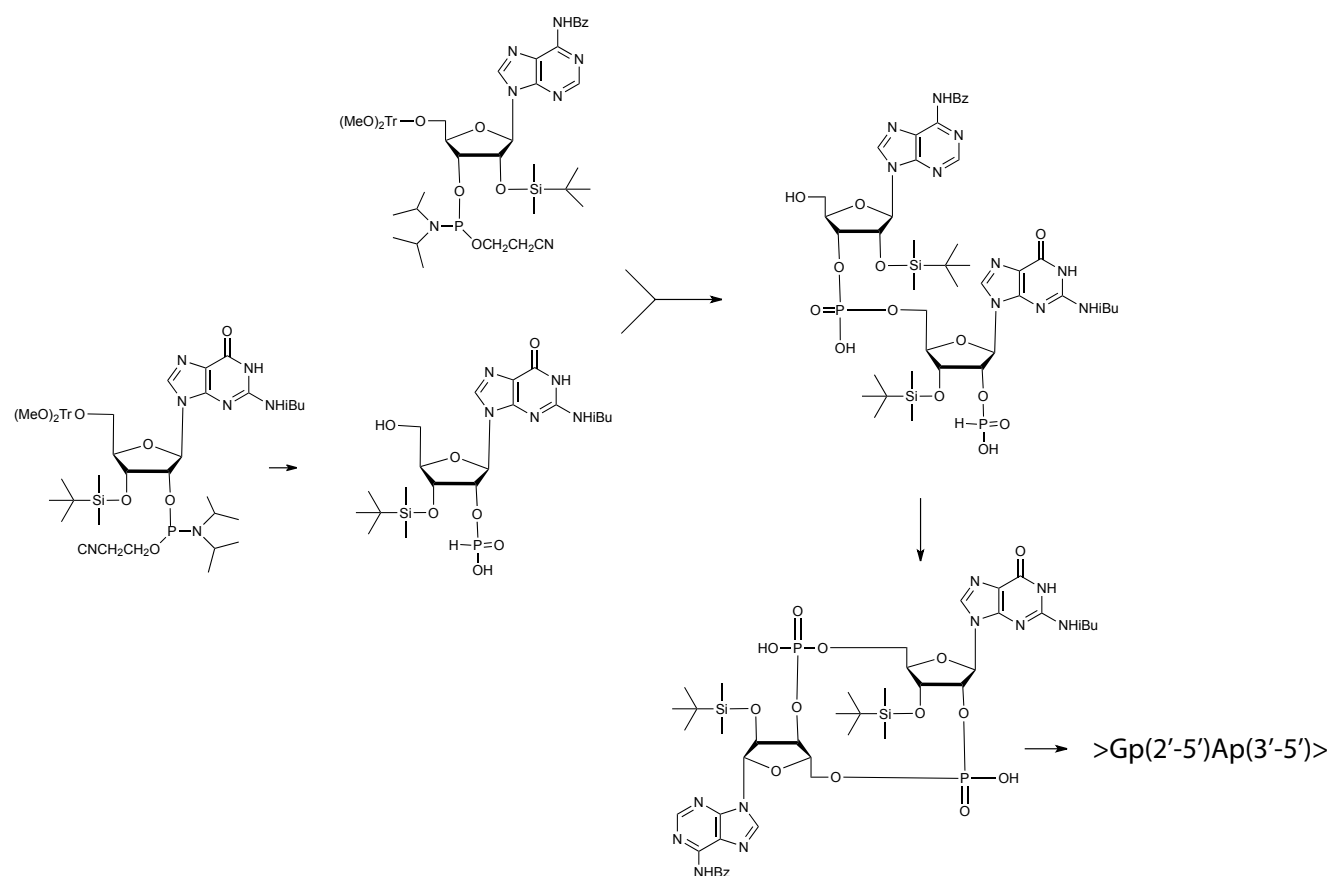
All in all, this partial assignment confirms that the cGAS reaction product contains 2'-phosphorylated guanosine and 3'-phosphorylated adenosine substructures, thereby clearly

supporting the result of enzymatic digestion experiments indicating the presence of >Gp(2'-5')Ap(3'-5')> linked ring structure.

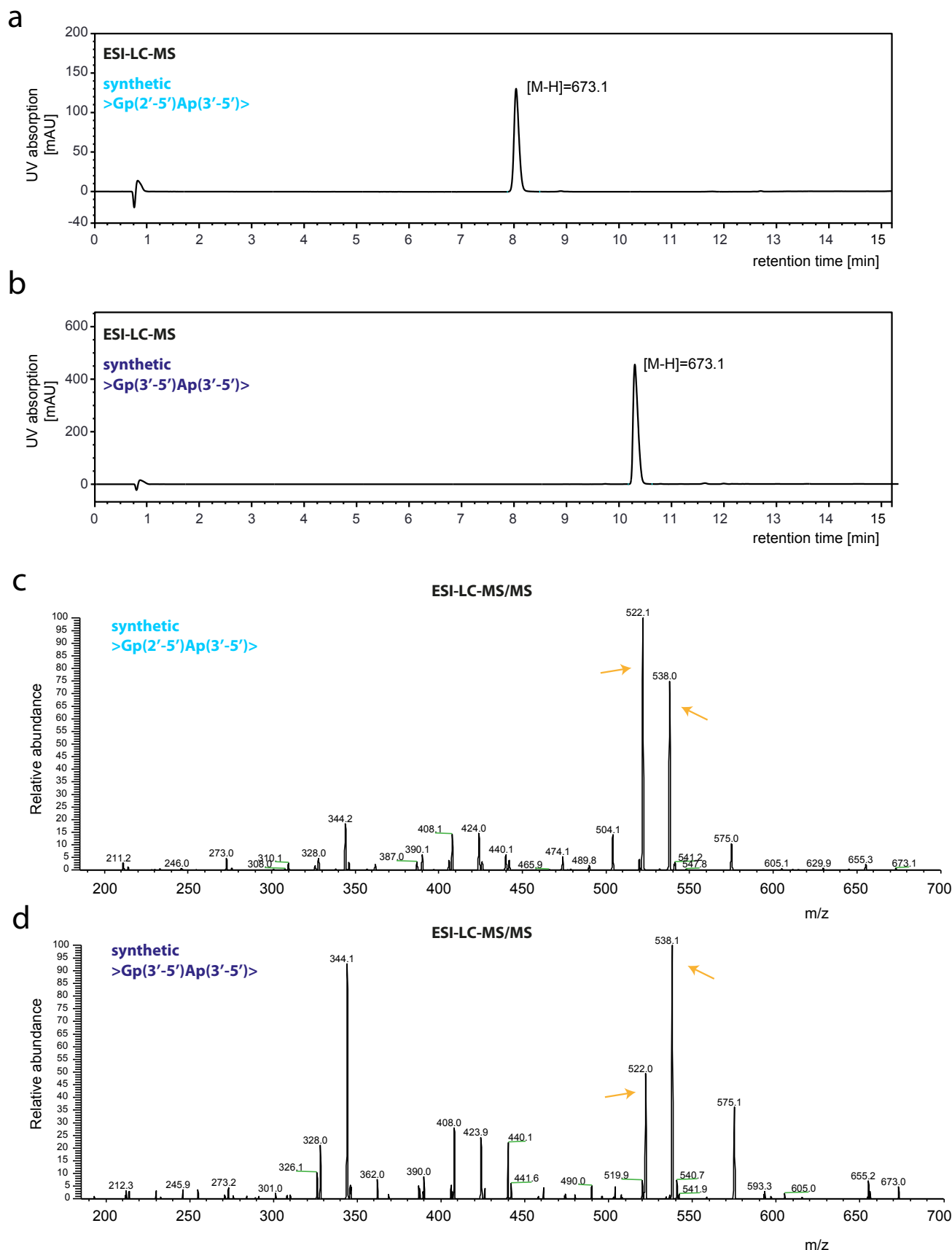
Based on these observations, a 3D structure model of cGAMP(2'-5') was generated by using the fragment based approach of COSMOS that relies on nucleotide structure parameters from crystallography databases⁸. The structure containing 2'-endo G ribose was selected based on the observed ¹H-NMR parameters for the conformation of the G ribose, and the adenine and guanine bases were rotated into trans orientation with Pymol to match the previously determined structure of cyclic-diGMP bound to STING by Yin et al. (4F9G.pdb)⁹.

References

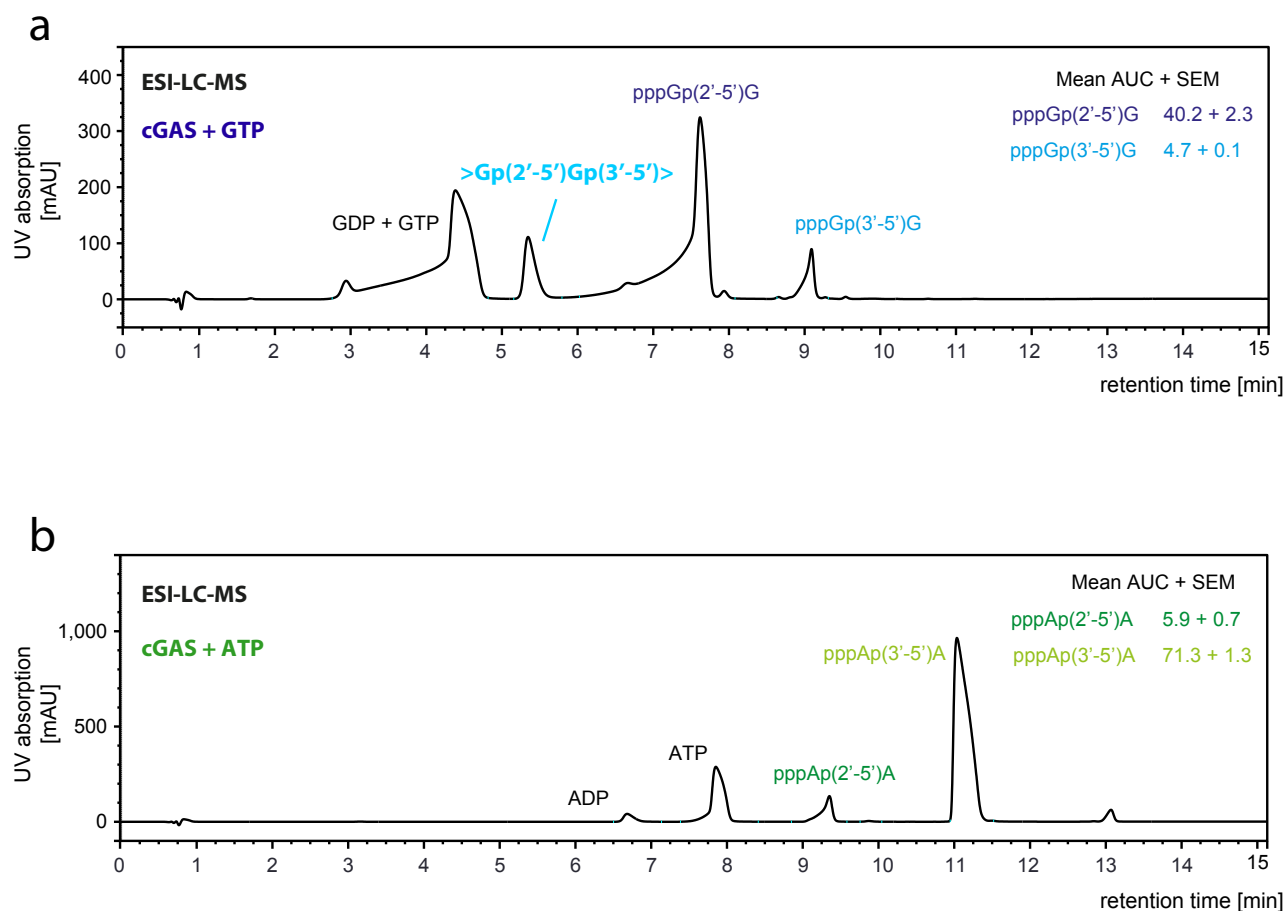
- 1 Gentner, M., Allan, M. G., Zaehring, F., Schirmer, T. & Grzesiek, S. Oligomer formation of the bacterial second messenger c-di-GMP: reaction rates and equilibrium constants indicate a monomeric state at physiological concentrations. *J Am Chem Soc* **134**, 1019-1029, doi:10.1021/ja207742q (2012).
- 2 Moreau, C. *et al.* Synthesis of cyclic adenosine 5'-diphosphate ribose analogues: a C2'endo/syn "southern" ribose conformation underlies activity at the sea urchin cADPR receptor. *Org Biomol Chem* **9**, 278-290, doi:10.1039/c0ob00396d (2011).
- 3 Altona, C. & Sundaralingam, M. Conformational analysis of the sugar ring in nucleosides and nucleotides. Improved method for the interpretation of proton magnetic resonance coupling constants. *J Am Chem Soc* **95**, 2333-2344 (1973).
- 4 Kellenberger, C. A., Wilson, S. C., Sales-Lee, J. & Hammond, M. C. RNA-Based Fluorescent Biosensors for Live Cell Imaging of Second Messengers Cyclic di-GMP and Cyclic AMP-GMP. *J Am Chem Soc*, doi:10.1021/ja311960g (2013).
- 5 Davies, D. B. & Danyluk, S. S. Nuclear magnetic resonance studies of 2'- and 3'-ribonucleotide structures in solution. *Biochemistry* **14**, 543-554 (1975).
- 6 Davies, D. B. & Danyluk, S. S. Nuclear magnetic resonance studies of 5'-ribo- and deoxyribonucleotide structures in solution. *Biochemistry* **13**, 4417-4434 (1974).
- 7 Sund, C., Agback, P., Koole, L. H., Sandström, A. & Chattopadhyaya, J. Assessment of competing 2'»5' versus 3'»5' stackings in solution structure of branched-RNA by ¹H- & ³¹P-NMR spectroscopy. *Tetrahedron* **48**, 695-718, doi:10.1016/S0040-4020(01)88130-8 (1992).
- 8 Andronico, A., Randall, A., Benz, R. W. & Baldi, P. Data-driven high-throughput prediction of the 3-D structure of small molecules: review and progress. *J Chem Inf Model* **51**, 760-776, doi:10.1021/ci100223t (2011).
- 9 Yin, Q. *et al.* Cyclic di-GMP sensing via the innate immune signaling protein STING. *Mol Cell* **46**, 735-745, doi:10.1016/j.molcel.2012.05.029 (2012)



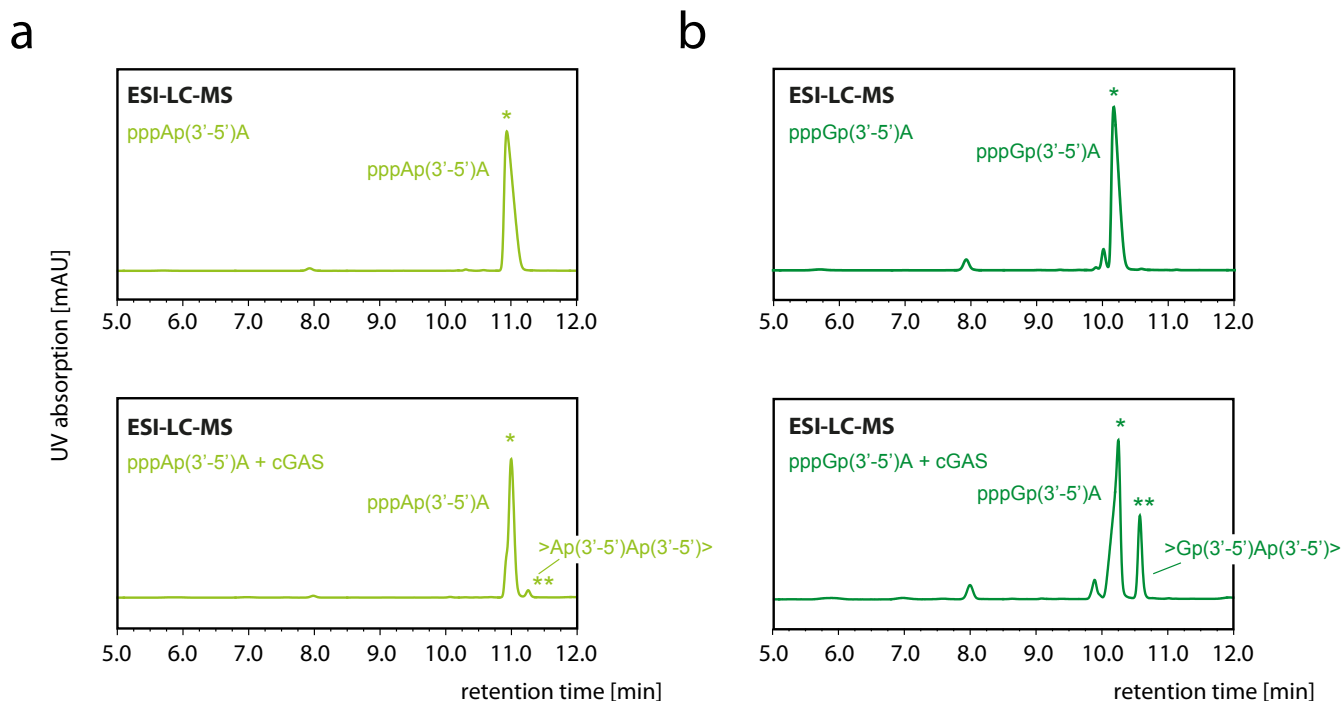
Supplementary Figure 12 | Chemical synthesis of cGAMP(2'-5'). Schematic overview of cGAMP(2'-5') chemical synthesis. A detailed protocol is described in the material and methods section.



Supplementary Figure 13 | LC-MS analysis of chemically synthesized cGAMP(2'-5') and cGAMP(3'-5').
(a-b) Chromatograms of chemically synthesized **(a)** cGAMP(2'-5') and **(b)** cGAMP(3'-5') are shown. **(c-d)**
Tandem MS spectra of the product peaks from **(a)** and **(b)** are depicted.



Supplementary Figure 14 | LC-MS analysis of cGAS enzymatic reaction products. (a-b) Chromatograms of in vitro cGAS enzymatic reaction products with (a) ATP or (b) GTP as only substrates are shown. The assignment of peaks to mono- and dinucleotide species was determined by LC-MS. In case of arguable isomers, characterization of the peaks was complemented with enzymatic digestion analysis for the crucial components. The insert on the upper right depicts the relative abundance of the two observed dinucleotide species. Data are representative of n=2 experiments.



Supplementary Figure 15 | The linear 3'-5' linked dinucleotides pppRp(3'-5')A are scarcely or not at all processed by cGAS. (a-b) Chromatograms before (top) and after (bottom) incubation of pppAp(3'-5')A (a) and pppGp(3'-5')A (b) with cGAS in in vitro enzymatic reactions are shown. Asterisks indicate the position of the substrates (*) and the resulting products (**), respectively. Data are representative of n=2 experiments.